PERGAMON

International Journal of Heat and Mass Transfer 43 (2000) 2739–2748

International Journal of HEAT and MASS TRANSFER

www.elsevier.com/locate/ijhmt

The conjugate conduction–natural convection heat transfer along a thin vertical plate with non-uniform internal heat generation

F Méndez[a], C Treviño[b,*]

[a]Facultad de Ingeniería, UNAM, 04510 México D.F., Mexico
[b]Facultad de Ciencias, UNAM, 04510 México D.F., Mexico

Received 15 December 1998; received in revised form 15 August 1999

Abstract

The steady state heat transfer characteristics of a thin vertical strip with internal heat generation is studied in this work. The nondimensional temperature distribution in the strip is obtained as a function of the following parameters: (a) the intensity and distribution of the internal heat sources, (b) the aspect ratio of the strip, (c) the longitudinal heat conductance of the strip and (d) the Prandtl number of the fluid. Both the thermally thin and the thick wall approximations are considered in this paper. The total thermal energy or averaged temperature of the strip is found to decrease as the influence of the longitudinal heat conduction effects in the strip decreases in the thermally thin wall regime. After reaching a minimum, it increases again in the thermally thick wall regime. © 2000 Elsevier Science Ltd. All rights reserved.

Keywords: Natural cooling; Heated slab; Conjugate heat transfer

1. Introduction

The fundamental studies of heat transfer processes with coupled effects of conduction and free or natural convection is extremely important because it appears in many practical and industrial devices, like building insulation, hot-film sensors, fin heat transfer, energy storage in enclosures, etc. However, the two mechanisms are generally decoupled and many works have appeared in the literature studying the natural convective heat transfer from vertical solid surfaces with prescribed surface temperature or heat flux. Since the classical analysis of Pohlhausen reported in the experimental paper of Schmidt and Beckmann [1], extensive studies of those pre-determined boundary conditions for the solid surfaces, have been developed in order to have a better knowledge of these processes. An excellent review can be found in Gebhart et al. [2]. However, a priori specification of temperature or heat transfer distribution at the wall represents a serious shortcoming of these analyses. In some cases, the conductive mechanisms in bounding walls directly coupled with the natural convective processes, have been analyzed in the literature. The natural convection boundary layer flow generated adjacent to a semi-infinite vertical slab of finite thickness was considered by Kelleher and Yang [3]. Similarly, Lock and Gunn [4]

* Corresponding author. Departmento DMT, Universidad Politécnica de Madrid, ESTI Aeronáuticos, Plaza del Cardenal Cisneros 3, 28040 Madrid, Spain.

0017-9310/00/$ - see front matter © 2000 Elsevier Science Ltd. All rights reserved.
PII: S0017-9310(99)00331-2

Nomenclature

c	specific heat of the natural fluid flow
c_w	specific heat of the strip
f	nondimensional stream function introduced in Eq. (5)
G_0	nondimensional temperature gradient, $G_0 = -d\phi_0/d\eta\|_0$
$G_1(n)$	nondimensional temperature gradient, $G_1(n) = -d\phi_{1n}/d\eta\|_0$
g	reduced nondimensional stream function introduced in Eq. (2)
g	acceleration of gravity
h	thickness of the strip
L	length of the strip
Pr	Prandtl number of the natural fluid flow
Ra_c	Rayleigh number of the natural fluid flow
T	temperature
T_∞	free stream temperature of the natural fluid flow
x, y	Cartesian coordinates
z	nondimensional normal coordinate of the strip defined in Eq. (4)

Greek symbols

α	heat conduction parameter, $\alpha = \lambda_w h/(\lambda L Ra^{1/4})$
δ	thickness of the natural boundary layer
ϕ	reduced nondimensional temperature introduced in Eq. (2)
ε	aspect ratio of the strip, $\varepsilon = h/L$
η	nondimensional normal coordinate for the natural fluid flow introduced in Eq. (4)
λ	thermal conductivity of the natural fluid flow
λ_w	plate thermal conductivity of the strip
ν	kinematic coefficient of viscosity of the natural fluid flow
ρ	density of the fluid
ρ_w	density of the strip
ξ	nondimensional coordinate introduced in Eq. (2)
θ	nondimensional temperature of the natural fluid flow introduced in Eq. (5)
θ_w	nondimensional temperature of the strip introduced in Eq. (5)
χ	nondimensional longitudinal coordinate defined in Eq. (4)

showed that the temperature distribution on a vertical flat plate is strongly influenced by the interaction with the adjacent boundary layer. Zinnes [5] studied the laminar boundary layer flow along a vertical flat plate with specified uniform heat flux at the surface, including the associated conductive transport in the plate. In this direction, Chen and Fang [6] using numerical methods, studied the conjugate problem along a vertical plate fin. Later, Vynnycky and Kimura [7] solved analytically and numerically the coupled elliptic governing equations for the conjugate free convection due to a vertical plate adjacent to a semi-infinite region. They confirmed that for high values of the Rayleigh number, the results give good agreement with a boundary layer formulation for the fluid phases. Merkin and Pop [8] analyzed the same problem with a boundary layer scheme and neglecting the axial heat conduction in the plate. They showed the influence of the Prandtl number for this conjugate free convection problem. Kimura et al. [9] studied experimentally the heat transfer process of a vertical heated slab. They developed a simple theory by assuming a uniform temperature at one surface of the slab. Clearly, the analysis does not reflect the experimental configuration, because the temperature itself is part of the solution of the conjugate heat transfer problem. Córdova and Treviño [10] clarified the role of the longitudinal heat transfer effects of a vertical thin plate in a natural convective cooling process and recently Treviño et al. [11] obtained similar results for a forced convective flow. They studied the thermally thin and thick wall regimes where simplifying assumptions can be employed to obtain approximate analytical solutions. Therefore, the importance of conjugated heat transfer problems is widely recognized in the literature and many different numerical and analytical methods have been applied for the above simple and conventional configurations. However in this general context, there are more complex situations, where the influence of other physical aspects like the electronic circuitry cooling with finite heat transfer generation rates, suggests new frontiers in conjugated heat problems. In these devices, the steady increase in the volumetric heat generation rates and the thermal management are decisive considerations in the design of chips with their packaging [12,13]. It is well known that the electronic behavior depends strongly on the temperature of the chip, the temperature gradients among the components and the associated thermal failures resulting from an overhigh chip temperature differences among the components related to critical electrical paths. Therefore, these failures are not to be only originated by irreversible mechanical fractures. This aspect was reported in Ref. [14]. In most applications, the thermal conditions on the electronic pack-

age surfaces are unknown and for a given heat generation rate, the temperature profiles within the heat source, including the location and the maximum values, are of primordial importance to obtain a high performance of the various electronic components within a specified range of temperatures. Several authors have pointed out these and related aspects, which can be found in Incropera [15] and Jaluria [16]. Later, Sathe and Joshi [17] showed the importance of the coupled heat transfer process between a heat generating substrate-mounted protrusion and a liquid-filled two-dimensional enclosure. In these works, the natural convection from discrete heat sources to extensive ambient air, is selected in comparison with other mechanisms of cooling. For simplicity, the flush heaters were idealized as uniform heat sources. On the other hand, several works have appeared in the literature to analyze the electronic cooling chip problem with forced flows. Recently, a well documented state of the art can be found in Cole [18].

Following the advantages of passive cooling mechanism by natural convection, which are characterized by simplicity of design, absence of noise and high reliability, the main objective of this work is to obtain, using asymptotic perturbation as well numerical techniques, the temperature distribution in a thin vertical embedded strip with non-uniform internal heat generation. For very large values of the Rayleigh number, Ra, to be defined later, a natural upstream boundary layer develops, causing a permanent heat transfer process controlled by the internal heat generation on the plate.

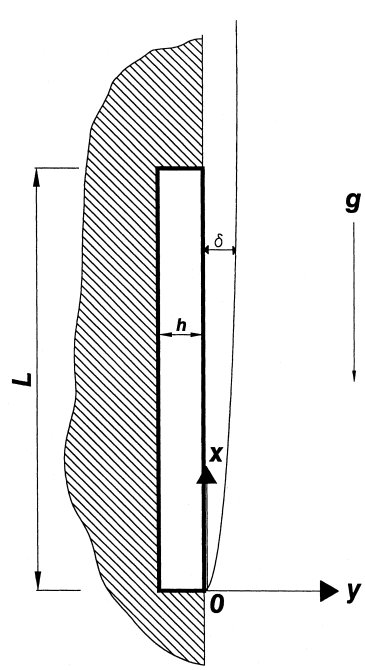

Fig. 1. Schematic of the heat transfer problem.

2. Order of magnitude analysis and formulation

Consider a vertical heat conducting strip of length L and thickness h, which is totally embedded in a vertical flat plate, except the right face of the strip which contacts a fluid with temperature T_∞ as shown in Fig. 1. Heat is generated internally with a non-uniform volumetric rate w. For simplicity, the left, upper and lower walls are supposed to be adiabatic. In order to satisfy it, the ratio of the thermal conductivity of the flat plate to the thermal conductivity of the strip is assumed to be vanishingly small compared with unity. There are many practical situations where it is a reasonable and well documented assumption [17]. In this simple case, the conjugated heat transfer process between the chip and the cooling flow is isolated. The lower right corner of the strip coincides with the origin of a Cartesian coordinate system whose y-axis points out in the normal direction to the plate and its x-axis points out in the plate's longitudinal direction. The temperature variations induce a natural convection flow due to the corresponding density changes. An order of magnitude analysis shows that these motions occur in boundary layers with thickness of order $L/Ra^{1/4}$, for large values of the Rayleigh number, $Ra = g\beta\Delta T Pr L^3/\nu^2$. Here, g is the acceleration of gravity, β and ν are thermal expansion coefficients and kinematic viscosities of the fluid. Pr denote the Prandtl number, $Pr = \rho\nu c/\lambda$, where ρ is the density, c is the specific heat and λ is the thermal conductivity of fluid, respectively. ΔT is the actual temperature difference across the fluid layer, which is in fact to be obtained from the analysis. After defining the Rayleigh number with a characteristic temperature difference, ΔT_c, to be defined later, $Ra_c = g\beta\Delta T_c Pr L^3/\nu^2$, the order of magnitude of the boundary layer thickness and the induced velocity are given by

$$\delta \sim \frac{L}{Ra_c^{1/4}}\left(\frac{\Delta T_c}{\Delta T}\right)^{1/4} \quad \text{and} \quad u_c \sim \frac{Ra_c^{1/2}\nu}{PrL}\left(\frac{\Delta T}{\Delta T_c}\right)^{1/2}. \tag{1}$$

The order of magnitude of the heat flux across the fluid is then

$$q \sim \frac{\lambda(\Delta T)^{5/4} Ra_c^{1/4}}{L(\Delta T_c)^{1/4}} \sim \frac{\lambda_w \Delta T_w}{h} \sim \bar{w}h. \tag{2}$$

In these relationships, ρ_w, c_w and λ_w represent the density, specific heat and thermal conductivity of the strip material. ΔT_w is the characteristic normal temperature drop at the strip and $\bar{w} = (1/L)\int_0^L w\,\mathrm{d}x$ is the averaged

volumetric heat production term. The last term in relation (2) arises from the thermal energy generated internally in the strip. From relationships (2), we obtain that ΔT_c must satisfy

$$\Delta T_c Ra_c^{1/4} \sim \frac{\bar{w}hL}{\lambda} = \Delta T^* \quad \text{and} \quad \frac{\Delta T_c}{\Delta T_w} \sim \frac{\alpha}{\varepsilon^2}. \tag{3}$$

Here ΔT^* is related to the heat generated internally. If we define the Rayleigh number as $Ra^* = Ra(\Delta T^*)$, then $Ra_c = (Ra^*)^{4/5}$ and $\Delta T_c = \Delta T^*/(Ra^*)^{1/5}$. ε is the aspect ratio of the strip, $\varepsilon = h/L$ and is to be assumed very small compared with unity. Parameter $\alpha = \lambda_w h/(\lambda L Ra_c^{1/4})$ is the nondimensional longitudinal heat conductance of the strip and corresponds to the ratio of the characteristic residence time in the fluid to the longitudinal diffusion time in the strip. α then gives the influence of the longitudinal heat conduction through the strip in the heat transfer process. This parameter can have values much larger or much smaller than unity, depending on the strip material. For values such as$\alpha/\varepsilon^2 \gg 1$, the temperature variations in the normal direction of the strip can be neglected, being very small, of order ε^2/α, compared with the temperature differences in the fluid. That is $\Delta T_w \ll \Delta T_c$. This regime is called the thermally thin wall regime. For values of $\alpha/\varepsilon^2 \sim 1$, the temperature variations in both directions of the strip now are very important and are of the same order of magnitude of the temperature differences in the fluid. This regime is called the thermally thick wall regime. In this regime because $\varepsilon \ll 1$, the longitudinal heat conduction through the strip is very small and can be neglected. Due to the singular character of the limit $\alpha \to 0$, the longitudinal heat conduction term is to be retained only in thin layers close to the vertical edges of the strip, in order to achieve the adiabatic boundary conditions. However, these thin heat conduction layers have only local influence. For reference, we notice here the correspondence $\omega = \sigma = \varepsilon^2/\alpha$ with the wall parameter ω of Anderson and Bejan [19] and the conjugate parameter σ of Kimura et al. [9].

In order to derive the nondimensional governing equations, we introduce the following nondimensional independent variables

$$\chi = \frac{x}{L}, \quad \eta = Ra_c^{1/4}\frac{y}{L\chi^{1/4}}, \quad z = \frac{y}{h}, \tag{4}$$

together with the nondimensional dependent variables

$$f = \frac{Pr\psi}{\nu Ra_c^{1/4}\chi^{3/4}}, \quad \theta = \frac{T - T_\infty}{\Delta T_c}, \quad \theta_w = \frac{T_w - T_\infty}{\Delta T_c}. \tag{5}$$

Here, ψ and f are the dimensional and non-dimensional stream functions defined in the usual way, respectively. The nondimensional balance equations, using the well-known Boussinesq and boundary layer approximations for large values of the Rayleigh number, then take the form

$$\frac{\partial^2\theta}{\partial\eta^2} + \frac{3}{4}f\frac{\partial\theta}{\partial\eta} = \chi\left(\frac{\partial f}{\partial\eta}\frac{\partial\theta}{\partial\chi} - \frac{\partial f}{\partial\chi}\frac{\partial\theta}{\partial\eta}\right) \tag{6}$$

$$\frac{\partial^3 f}{\partial\eta^3} + \theta = \frac{1}{Pr}\left[\frac{1}{2}\left(\frac{\partial f}{\partial\eta}\right)^2 - \frac{3}{4}f\frac{\partial^2 f}{\partial\eta^2} + \chi\left(\frac{\partial f}{\partial\eta}\frac{\partial^2 f}{\partial\chi\partial\eta} - \frac{\partial f}{\partial\chi}\frac{\partial^2 f}{\partial\eta^2}\right)\right], \tag{7}$$

for the fluid and

$$\alpha\frac{\partial^2\theta_w}{\partial\chi^2} + \frac{\alpha}{\varepsilon^2}\frac{\partial^2\theta_w}{\partial z^2} + \frac{w}{\bar{w}} = 0, \tag{8}$$

for the strip. The boundary conditions are given by

$$f = \frac{\partial f}{\partial\eta} = \theta - \theta_w = \frac{\partial\theta_w}{\partial z} - \frac{\varepsilon^2}{\alpha\chi^{1/4}}\frac{\partial\theta}{\partial\eta} = 0 \quad \text{at } \eta = z = 0 \tag{9}$$

$$\frac{\partial\theta_w}{\partial z} = 0 \quad \text{at } z = -1 \tag{10}$$

$$\frac{\partial\theta_w}{\partial\chi} = 0 \quad \text{for } \chi = 0 \text{ and } \chi = 1 \tag{11}$$

$$\frac{\partial f}{\partial\eta} = \theta = 0 \quad \text{for } \eta \to \infty. \tag{12}$$

In general, this system of elliptic equations can be numerically integrated. In the following section we explore asymptotic solutions in both, the thermally thin and thick wall regimes.

3. Thermally thin wall regime

As mentioned before, for very large values of α/ε^2 compared with unity, the temperature variations in the normal direction in the strip can be neglected and the nondimensional temperature is, in a first approximation, only a function of the longitudinal coordinate χ. In this regime the characteristic diffusion time in the normal direction $h^2\rho_w c_w/\lambda_w$ is very small compared with the residence time L/u_c. Thus, the integral form of the nondimensional energy equation for the strip (8) can be obtained by integrating along the normal coordinate and after applying the boundary conditions (9) and (10), we get

$$\alpha\frac{d^2\theta_w}{d\chi^2} = -\frac{w}{\bar{w}} - \frac{1}{\chi^{1/4}}\frac{\partial\theta}{\partial\eta}\bigg|_{\eta=0}. \tag{13}$$

This equation must be solved with the adiabatic conditions for the lateral surfaces of the strip given by Eq. (11). In the following subsection we present the asymptotic solution for $\alpha \gg 1$, for this thermally thin wall regime. For values of α of order unity, the problem must be solved numerically.

3.1. Asymptotic limit $\alpha \gg 1$

From the physical point of view the temperature variations in the normal direction are negligible compared with the corresponding temperature differences in the fluid. This fact was deduced by an order of magnitude analysis in the previous section for the thermally wall regime, through relationship (3). Large values of the parameter α can be obtained by increasing the thermal conductivity and the aspect ratio of the strip. In this limit, the non-dimensional temperature of the plate changes very little in the longitudinal direction, of order α^{-1}. For a thermally thin wall, this conjugate heat transfer problem can be studied in the asymptotic limit $\alpha\rightarrow\infty$, assuming the following expansion

$$\theta_w = \sum_{j=0}^{\infty}\frac{1}{\alpha^j}\theta_{wj}(\chi), \qquad \Omega = \sum_{j=0}^{\infty}\frac{1}{\alpha^j}\Omega_j(\chi,\eta) \tag{14}$$

with Ω corresponding to any property of the fluid, like f or θ. Introducing the above relationships (14) into the non-dimensional governing Eq. (13) for the plate, we obtain the following set of equations

$$\frac{d^2\theta_{w0}}{d\chi^2} = 0, \quad \frac{d^2\theta_{w1}}{d\chi^2} = -\frac{w}{\bar{w}} - \frac{1}{\chi^{1/4}}\frac{\partial\theta_0}{\partial\eta}\bigg|_0$$

$$\frac{d^2\theta_{wj}}{d\chi^2} = -\frac{1}{\chi 1/4}\frac{\partial\theta_{j-1}}{\partial\eta}\bigg|_0 \quad \text{for all } j > 1. \tag{15}$$

The problem is to be solved with the following adiabatic boundary conditions

$$\frac{d\theta_{wj}}{d\chi} = 0 \quad \text{at } \chi = 0, 1 \text{ for all } j. \tag{16}$$

The leading order variable θ_{w0} must be a constant to be determined below. This value can be found after integrating the first order equation (15), with the corresponding adiabatic conditions at both edges, giving $d\theta_0/d\eta|_{\eta=0} = -3/4$. The solution of the leading order equations for the fluid (see the Appendix for details) are self-similar and can be readily obtained as [20]

$$\frac{d\theta_0}{d\eta}|_{\eta=0} = -G_0\theta_{w0}^{5/4} = -\frac{3}{4}, \tag{17}$$

where G_0 is the fluid nondimensional temperature gradient at the strip for the normalized case and is given by

$$G_0(Pr) \approx \frac{3}{4}\left[\frac{2Pr/5}{1+2Pr^{1/2}+2Pr}\right]^{1/4}. \tag{18}$$

Thus, the leading order solution for the nondimensional temperature of the strip is

$$\theta_{w0} = \left[\frac{3}{4G_0(Pr)}\right]^{4/5}. \tag{19}$$

Introducing the solution for θ_{w0} into the first order equation (15) for θ_{w1}, this takes the form

$$\frac{d^2\theta_{w1}}{d\chi^2} = -\frac{w}{\bar{w}} + \frac{G_0\theta_{w0}^{5/4}}{\chi^{1/4}}, \tag{20}$$

with the boundary conditions given by Eq. (16). The solution to this equation is given by

$$\theta_{w1} = b_0 + b_{7/4}\chi^{7/4} + b_{m+2}\chi^{m+2}, \tag{21}$$

where b_0 is to be obtained from the second-order equation (15), $b_{7/4} = 4/7$ and $b_{m+2} = -1/(m+2)$. In this case we represented for simplicity the normalized internal heat production function $w/\bar{w}$ as $w/\bar{w} = (1+m)\chi^m$. The exponent m then represents the distribution of the internal heat sources in the strip. $m = 0$ yields a spatially uniform function and $m > 0$ generates functions that rise monotonically along the plate and for larger values of m, shifts the distributions towards $\chi = 1$.

Integrating Eq. (15) for $j = 2$ and applying the adiabatic boundary conditions at both edges, we obtain

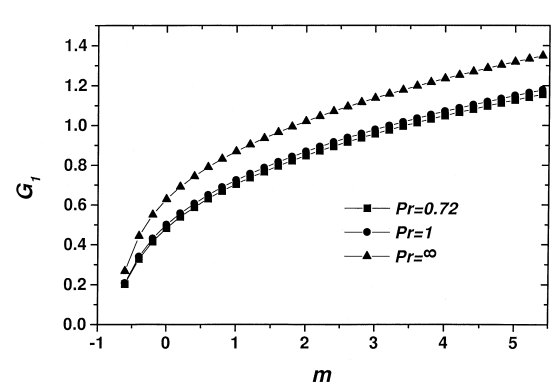

Fig. 2. Values of the nondimensional temperature gradients $G_1(n, Pr)$ as a function of n, for different values of the Prandtl number, $Pr = 0.72$, 1 and ∞.

$$\int_0^1 \frac{d^2\theta_{w2}}{d\chi^2} d\chi = -\int_0^1 \frac{\partial\theta_1}{\partial\eta}|_0 \frac{d\chi}{\chi^{1/4}} = 0. \tag{22}$$

In the Appendix we show that the nondimensional gradient of the first order solution is given by

$$\frac{\partial\theta_1}{\partial\eta}|_0 = -\theta_{w0}^{1/4} \sum_{n=0,\ 7/4,\ m+2} b_n \chi^n G_1(n). \tag{23}$$

Introducing Eq. (23) in (22) we obtain the value of the constant b_0 as

$$b_0 = \frac{3}{4G_1(0)}\left[\frac{G_1(m+2)}{(m+2)(m+11/4)} - \frac{8}{35}G_1(7/4)\right]. \tag{24}$$

The functions $G_1(n)$ are obtained after solving the following linear set of ordinary differential equations for the boundary layer equations (see Appendix). Fig. 2 shows G_1 as a function of n and three different values of the Prandtl number, $Pr = 0.72$, 1 and ∞. Similar to G_0, G_1 is a monotonic increasing function with Pr and m.

The averaged nondimensional temperature, up to terms of order $1/\alpha$, is then given by

$$\begin{aligned}\bar{\theta}_w &= \int_0^1 \theta_w d\chi \simeq \theta_{w0} + \frac{1}{\alpha}\bar{\theta}_{w1} \\ &= \theta_{w0} + \frac{1}{\alpha}\left\{\frac{3}{4G_1(0)}\left[\frac{G_1(m+2)}{(m+2)(m+11/4)}\right.\right. \\ &\quad \left.\left. - \frac{8}{35}G_1(7/4)\right] + \frac{16}{77} - \frac{1}{(m+2)(m+3)}\right\}.\end{aligned} \tag{25}$$

For $Pr = 1$, an excellent correlation gives

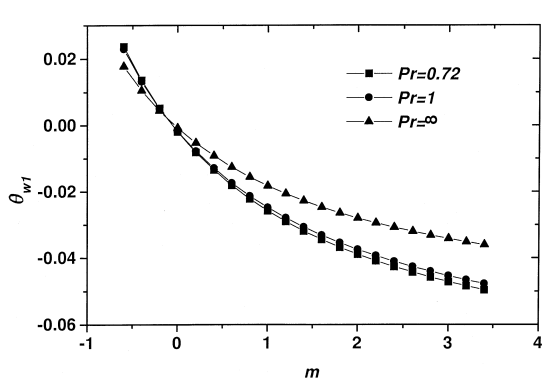

Fig. 3. First order solution for the nondimensional overall thermal energy of the strip for the thermally thin wall regime, as a function of the distribution parameter m, for different values of the Prandtl number.

$$\begin{aligned}\bar{\theta}_w \simeq 1.6572 &+ \frac{1}{\alpha}\left[-0.00174 - 0.03244m\right. \\ &\left. + 0.01182m^2 - 0.00286m^3 + 0.0003m^4\right] \\ &+ O(\alpha^{-2}).\end{aligned} \tag{26}$$

Fig. 3 shows $\bar{\theta}_{w1}$ as a function of the distribution parameter m for three different values of the Prandtl number. For positive values of m, this function is always negative, showing that the overall thermal energy of the plate decreases with decreasing values of α in the thermally thin wall regime.

3.2. Asymptotic limit $\alpha \to 0$

The limiting behavior in this regime is obtained in the limit $\alpha \to 0$, but with $\alpha/\varepsilon^2 \gg 1$. In this case the longitudinal heat conduction in the strip is very small and can be neglected except in regions close to the edges of the plate. From Eq. (13) with $\alpha = 0$, we obtain

$$\left.\frac{\partial\theta}{\partial\eta}\right|_{\eta=0} = -\frac{w}{\bar{w}}\chi^{1/4} = -(1+m)\chi^{m+1/4}. \tag{27}$$

With this known heat flux distribution, the fluid governing Eqs. (6) and (7) and the nondimensional temperature of the plate (Eq. (8)) with the corresponding boundary conditions can be solved with a simple scheme. Using the invariance property of the boundary layer equations shown in the Appendix, we introduce the following variables

$$\eta = \chi^s\tilde{\eta}, \quad f = \chi^t\tilde{f}, \quad \theta = \chi^r\tilde{\theta}(\tilde{\eta}) \quad \text{and } \theta_w = \chi^r\tilde{\theta}(0). \tag{28}$$

It can be easily shown that for this case

$$r = \frac{4m+1}{5}, \quad s = -t = -\frac{m+1/4}{5}, \tag{29}$$

and the problem of the fluid is reduced to solve a conventional heat transfer problem with a known uniform heat flux distribution at the surface of the wall. Therefore, the nondimensional temperature of the plate is given by

$$\theta_w = \tilde{\theta}(0)\chi^{(4m+1)/5}, \tag{30}$$

and $\tilde{\theta}(0)$ is to be obtained from solving the nonlinear set of ordinary differential equations

$$\frac{d^2\tilde{\theta}}{d\tilde{\eta}^2} + \frac{m+4}{5}\frac{d\tilde{\theta}}{d\tilde{\eta}}\tilde{f} - \frac{(4m+1)}{5}\tilde{\theta}\frac{d\tilde{f}}{d\tilde{\eta}} = 0 \tag{31}$$

$$\frac{d^3\tilde{f}}{d\tilde{\eta}^3}+\tilde{\theta}=\frac{1}{Pr}\left[\frac{(2m+3)}{5}\left(\frac{d\tilde{f}}{d\tilde{\eta}}\right)^2-\frac{(m+4)}{5}\tilde{f}\frac{d^2\tilde{f}}{d\tilde{\eta}^2}\right] \tag{32}$$

with the boundary conditions

$$\frac{d\tilde{\theta}}{d\tilde{\eta}}+(1+m)=\tilde{f}=\frac{d\tilde{f}}{d\tilde{\eta}}=0 \quad \text{at } \tilde{\eta}=0 \tag{33}$$

$$\tilde{\theta}=\frac{d\tilde{f}}{d\tilde{\eta}}=0 \quad \text{for } \tilde{\eta}\to\infty. \tag{34}$$

In Fig. 4 $\tilde{\theta}(0)$ is shown as a function of m, for three different values of the Prandtl number. It represents the nondimensional temperature at $\chi=1$. It means that the maximum temperature at the strip is achieved for increasing values of m. However, the averaged nondimensional temperature

$$\bar{\theta}_w=\frac{5}{4m+6}\tilde{\theta}(0), \tag{35}$$

decreases with m. $\bar{\theta}_w$ is also plotted in Fig. 4 for different values of the Prandtl number.

4. Thermally thick wall regime

In this regime, the longitudinal heat conduction is also very small and is to be neglected. The energy balance equation for the plate (Eq. (8)) then reduces to

$$\frac{\partial^2\theta_w}{\partial z^2}=-\frac{\varepsilon^2}{\alpha}(1+m)\chi^m. \tag{36}$$

Eq. (36) has to be solved with the boundary conditions:

$$\frac{\partial\theta_w}{\partial z}=0 \quad \text{at } z=-1, \quad \frac{\partial\theta_w}{\partial z}=\frac{\varepsilon^2}{\alpha\chi^{1/4}}\frac{\partial\theta}{\partial\eta} \quad \text{at } \eta=z=0. \tag{37}$$

Integrating Eq. (36) in the normal z-direction and applying the boundary conditions (37), we obtain

$$\frac{\partial\theta}{\partial\eta}|_0=-(1+m)\chi^{m+1/4}, \tag{38}$$

which is independent of ε and α. The nondimensional temperature of the plate is then

$$\theta_w=\theta_{wu}-\frac{(1+m)\varepsilon^2}{\alpha}\chi^m\left(z+z^2/2\right), \tag{39}$$

where θ_{wu} is the nondimensional temperature at the upper surface of the plate $\theta_{wu}=\tilde{\theta}(0)\chi^{(4m+1)/5}$ and is exactly the same as that obtained for the thermally thin wall regime. The averaged nondimensional temperature is then

$$\bar{\theta}_w=\frac{5}{4m+6}\tilde{\theta}(0)+\frac{1}{3}\frac{\varepsilon^2}{\alpha}. \tag{40}$$

In the limit of $\varepsilon^2/\alpha\to 0$, the total thermal energy of the strip in this regime is exactly the same as for the case of $\alpha\to 0$, for the thermally thin wall regime given by Eq. (35).

5. Results and discussion

In order to validate the analytical results, the system of equations for the thermally thin wall regime were integrated numerically using the quasi-linearization technique for the boundary layer equations and the integrated form of the strip equation (13). The bound-

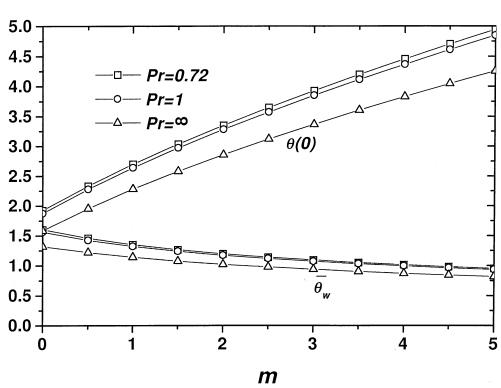

Fig. 4. Solution for the asymptotic limit of $\alpha=0$ for the thermally thin wall regime. The functions $\tilde{\theta}(0)$ and the nondimensional overall thermal energy of the strip $\bar{\theta}_w$ as a function of the distribution parameter m, for different values of the Prandtl number.

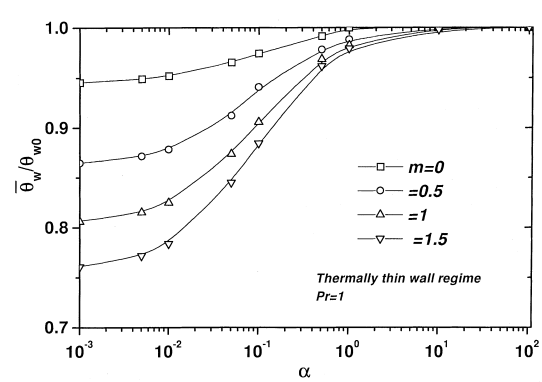

Fig. 5. Numerical solution for the normalized overall thermal energy of the strip as a function of α, for different values of the distribution parameter m. The calculations were done for a Prandtl number, $Pr=1$.

ary conditions in the fluid for $\eta \to \infty$ uses a finite mesh point, η_∞, chosen by making numerical experiments by increasing η_∞ until a non-significant change in the solution is obtained (for $Pr = 1$, $\eta_\infty = 9$ produces an error in the solution less than 1×10^{-10}). The solution of the governing equations for the case of $Pr \to \infty$ was obtained using the boundary condition $\partial^2 f/\partial\eta^2 = 0$ instead of $\partial f/\partial\eta = 0$ at $\eta = \eta_\infty$. Because the non linearity of the boundary layer equations, it was necessary to implement an iterative method based on the introduction of a pseudo-transient term in Eq. (13), with a convergence parameter lower than 1×10^{-10}. The mesh used for the balance equations were 200×200, for the longitudinal and normal directions and a pseudo-time step not larger than 0.01.

Figs. 5 and 6 show the numerical calculations with $Pr = 1$ and $\varepsilon = 0.1$ for the normalized overall nondimensional thermal energy of the strip $\bar{\theta}_w/\theta_{w0}$ as a function of α/ε^2. In Fig. 5, we plot the corresponding results for the thermally thin wall regime. For large values of α, the temperature of the plate is independent of m. However, as the value of α decreases, the overall thermal energy of the strip decreases and this is amplified for increasing values of m as was anticipated in Eq. (25). As α reaches values of order ε^2, the overall thermal energy of the strip reaches practically a minimum value. In Fig. 6 we show the numerical results for the thermally thin wall regime compared with the analytical results for the thermally thin and thick wall regimes, for $m = 0$. For large values of α, the asymptotic solution obtained in the limit $\alpha \to \infty$, given by Eq. (25), provides accurate results for values of $\alpha > 0.5$. As the value of α decreases further, the solution in the thermally thin wall regime reaches asymptotically the solution deduced for $\alpha \to 0$. However, for values of α of order ε^2, the thermally thin wall regime is not more appropriate and the averaged temperature of the strip will increase with decreasing values of α. The solution then becomes closer to the analytical solution obtained for the thermally thick wall regime given by Eq. (40). The minimum value of the overall thermal energy is not predicted by the thermally thin and thick wall regimes. The minimum value is produced in the transition region from thin to thick wall regimes and can be obtained by solving the full energy equation for the strip.

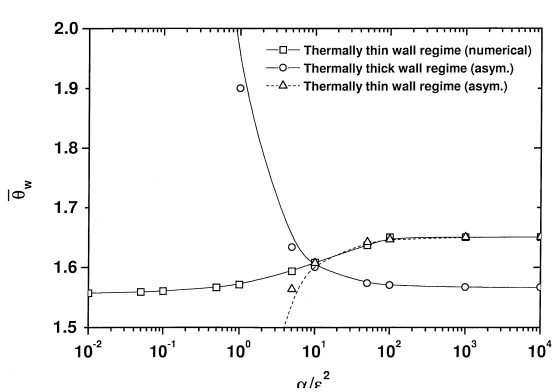

Fig. 6. Numerical solution for the normalized overall thermal energy of the strip as a function of α for $m = 0$, $Pr = 1$, for the thermally thin wall regime. The analytical solutions for the thermally thin and thick wall regimes given by Eqs. (25) and (40) respectively, are also plotted with a value of $\varepsilon = 0.1$.

Fig. 7 shows the nondimensional temperature distribution θ_w as a function of the normalized longitudinal coordinate χ, for different values of the parameter α. The calculations were done with $Pr = 1$ and $m = 0$ for the thermally thin wall regime. The temperature is almost flat for values of $\alpha \geq 1$. For smaller values of α, the temperature decreases strongly at the upper end of the plate and increases at the lower end.

As illustration, a numerical computation was performed using air as the cooling fluid at $T_\infty = 300$ K. The numerical data of the thermal properties was taken from Sathe [17] and Incropera [21]. Using a strip of 5 cm length, 0.5 cm thickness, with a volumetric heat production rate of 40 kW/m^3, we obtain the following values for the important parameters: $\Delta T^* = 381.1$ K, $\Delta T_c = 17.7$ K, $Ra^* = 4.56 \times 10^6$, $Ra_c = 2.12 \times 10^5$ and thus $\alpha = 0.465$ and $\alpha/\varepsilon^2 = 46.5$. With this value of α and using Fig. 6, we obtain $\bar{\theta}_w \simeq 1.63$. Remembering that $\bar{T}_w = T_\infty + \Delta T_c \bar{\theta}_w$, the average temperature of the strip in physical units is $\bar{T}_w \sim 328.9$ K. In this numerical case, the limit of thermally thin flat plate prevails with a value of $\alpha \sim 1$. The expected temperature gradient in the streamwise direction of the strip is, using Eq. (21), $\Delta T_c/(14\alpha L) \sim 5.4$ K/cm. The resulting value of the temperature gradient shows that natural cooling process must be used with caution to avoid large thermal stresses, insofar as the strip is embedded in a material with a very different

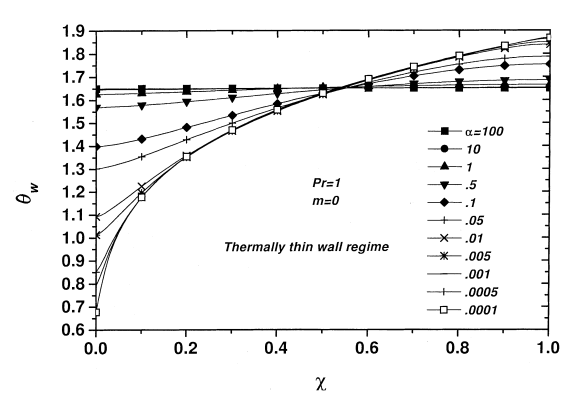

Fig. 7. Numerical solution for the nondimensional temperature of the strip as a function of χ, for different values of α.

thermal conductivity. A better operation condition can be obtained by increasing the value of α, in order to reach lower values of the temperature gradient.

Acknowledgements

This work has been supported by the research grant IN107795, DGAPA at UNAM, Mexico. We also thank E. Luna for his help in the numerical computations.

Appendix

In this appendix we derive the asymptotic solution for the boundary layer governing equations for the limit $\alpha \to \infty$. Due to the fact that the boundary layer Eqs. (6) and (7) are invariant under the group of transformation

$$\theta \Longrightarrow B\theta, \quad \eta \Longrightarrow B^{-1/4}\eta, \quad f \Longrightarrow B^{1/4} f, \tag{A1}$$

it is convenient to normalize the variables at least for the leading term equations. Introducing the new variables

$$\theta = \theta_{w0}\phi, \quad \eta = \theta_{w0}^{-1/4}\xi \quad \text{and} f = \theta_{w0}^{1/4} g, \tag{A2}$$

the boundary layer equations now take the form

$$\frac{\partial^3 g}{\partial \xi^3} + \phi = \frac{1}{Pr}\left\{\chi\left[\frac{\partial g}{\partial \xi}\frac{\partial^2 g}{\partial \chi \partial \xi} - \frac{\partial g}{\partial \chi}\frac{\partial^2 g}{\partial \xi^2}\right] + \frac{1}{2}\left[\frac{\partial g}{\partial \xi}\right]^2 - \frac{3}{4} g \frac{\partial^2 g}{\partial \xi^2}\right\} \tag{A3}$$

$$\frac{\partial^2 \phi}{\partial \xi^2} + \frac{3}{4} g \frac{\partial \phi}{\partial \xi} = \chi\left[\frac{\partial g}{\partial \xi}\frac{\partial \phi}{\partial \chi} - \frac{\partial g}{\partial \chi}\frac{\partial \phi}{\partial \xi}\right]. \tag{A4}$$

Assuming a series solution of the form

$$\phi = \sum_{j=0}^{\infty} \frac{1}{\alpha^j}\phi_j(\chi, \xi) \quad \text{and} \quad g = \sum_{j=0}^{\infty} \frac{1}{\alpha^j} g_j(\chi, \xi), \tag{A5}$$

the leading term form of the boundary layer equations reduce to the classical constant temperature case given by

$$\frac{d^3 g_0}{d\xi^3} + \phi_0 = \frac{1}{Pr}\left\{\frac{1}{2}\left[\frac{dg_0}{d\xi}\right]^2 - \frac{3}{4} g_0 \frac{d^2 g_0}{d\xi^2}\right\} \tag{A6}$$

$$\frac{d^2 \phi_0}{d\xi^2} + \frac{3}{4} g_0 \frac{d\phi_0}{d\xi} = 0, \tag{A7}$$

with the boundary conditions

$$\phi_0 - 1 = \frac{dg_0}{d\xi} = g_0 = 0 \quad \text{at } \xi = 0 \tag{A8}$$

$$\frac{dg_0}{d\xi} = \phi_0 = 0 \quad \text{for } \xi \to \infty. \tag{A9}$$

The solution to these Eqs. (A6)–(A9) can be found elsewhere [20] and the nondimensional temperature gradient at the wall is then given by a very good correlation

$$\frac{d\phi_0}{d\xi}|_{\xi=0} = -G_0(Pr) \approx -\frac{3}{4}\left[\frac{2Pr}{5(1 + 2Pr^{1/2} + 2Pr)}\right]^{1/4}. \tag{A10}$$

Integrating twice Eq. (20), gives that θ_{w1} can be represented by the summation of three terms

$$\theta_{w1} = \sum_{n=0,\ 7/4,\ m+2} b_n \chi^n. \tag{A11}$$

Therefore, g_1 and ϕ_1 can also be written as

$$g_1 = \sum_{n=0,\ 7/4,\ m+2} \frac{b_n}{\theta_{w0}} \chi^n g_{1n}, \qquad \phi_1 = \sum_{n=0,\ 7/4,\ m+2} \frac{b_n}{\theta_{w0}} \chi^n \phi_{1n}, \tag{A12}$$

where g_{1n} and ϕ_{1n} satisfy the following normalized linear equations

$$\frac{d^3 g_{1n}}{d\xi^3} + \phi_{1n} + \frac{1}{Pr_i}\left\{-(1+n)\frac{dg_0}{d\xi}\frac{dg_{1n}}{d\xi} + \left(\frac{3}{4} + n\right) g_{1n}\frac{d^2 g_0}{d\xi^2} + \frac{3}{4} g_0 \frac{d^2 g_{1n}}{d\xi^2}\right\} = 0 \tag{A13}$$

$$\frac{d^2 \phi_{1n}}{d\xi^2} + \frac{3}{4} g_0 \frac{d\phi_{1n}}{d\xi} + \frac{3}{4} g_{1n}\frac{d\phi_0}{d\xi} - n\left[\frac{dg_0}{d\xi}\phi_{1n} - g_{1n}\frac{d\phi_0}{d\xi}\right] = 0 \tag{A14}$$

with the normalized boundary conditions

$$\phi_0 - 1 = \phi_{1n} - 1 = g_0 = g_{1n} = \frac{dg_0}{d\xi} = \frac{dg_{1n}}{d\xi} = 0 \quad \text{at } \xi = 0 \tag{A15}$$

$$\frac{dg_0}{d\xi} = \frac{dg_{1n}}{d\xi} = \phi_0 = \phi_{1n} = 0 \quad \text{for } \xi \to \infty. \tag{A16}$$

The nondimensional heat flux $\partial\theta/\partial\eta|_0$ is then, up to the first order in α

$$\frac{\partial\theta}{\partial\eta}|_0 = \theta_{w0}^{5/4}\frac{\partial\phi}{\partial\xi}|_0 = \theta_{w0}^{5/4}\frac{\mathrm{d}\phi_0}{\mathrm{d}\xi}|_0 + \frac{\theta_{w0}^{1/4}}{\alpha}\sum_{n=0,\ 7/4,\ m+2} b_n\chi^n\frac{\mathrm{d}\phi_{1n}}{\mathrm{d}\xi}|_0 + O(\alpha^{-2}) \tag{A17}$$

or

$$\frac{\partial\theta}{\partial\eta}|_0 = -\theta_{w0}^{5/4}G_0 - \frac{\theta_{w0}^{1/4}}{\alpha}\sum_{n=0,\ 7/4,\ m+2} b_n\chi^n G_1(n) + O(\alpha^{-2}), \tag{A18}$$

where

$$G_1(n) = -\frac{\mathrm{d}\phi_{1n}}{\mathrm{d}\eta}|_0.$$

References

[1] E. Schmidt, W. Beckmann, E. Pohlhausen, Das Temperatur- und Geschwindigkeitsfeld von einer wärme abgebenden, senkrechten Platte bei natürlicher Konvektion, Forschg. Ing.-Wes 1 (1930) 391–404.

[2] B. Gebhart, Y. Jaluria, R.L. Mahajan, B. Sammakia, Bouyancy-Induced Flows and Transport, Hemisphere, NY, 1988.

[3] M. Kelleher, K.T. Yang, A steady conjugate heat transfer problem with conduction and free convection, Appl. Sci. Res 17 (1967) 249–269.

[4] G.S.H. Lock, J.C. Gunn, Laminar free convection from a downward-projecting fin, J. Heat Transfer 90 (1968) 63–70.

[5] A.E. Zinnes, The coupling of conduction with laminar convection from a vertical flat plate with arbitrary surface heating, ASME J. Heat Transfer 92 (1970) 528–535.

[6] H.T. Chen, L.C. Fang, Simple computational method for conjugate conduction-natural convection along a vertical plate fin, Engineering Analysis with Boundary Elements 10 (1992) 93.

[7] M. Vynnycky, S. Kimura, Conjugate free convection due to a heated vertical plate, International Journal of Heat and Mass Transfer 39 (1996) 1067–1080.

[8] J.H. Merkin, I. Pop, Conjugate free convection on a vertical surface, International Journal of Heat and Mass Transfer 39 (1996) 1527–1534.

[9] S. Kimura, A. Okajima, T. Kiwata, Conjugate natural convection from a vertical heated slab, International Journal of Heat and Mass Transfer 41 (1998) 3203–3211.

[10] J. Córdova, C. Treviño, Effects of longitudinal heat conduction of a vertical thin plate in a natural convective cooling process, Wärme- und Stoffübertragung 29 (1994) 195–204.

[11] C. Treviño, G. Becerra, F. Méndez, On the classical problem of a convective heat transfer on a laminar flow from a thin finite thickness plate with uniform temperature, International Journal of Heat and Mass Transfer 40 (1997) 3577–3580.

[12] K.W. Tou, G.P. Xu, C.P. Tso, Direct liquid cooling of electronic chips by single-phase forced convection of FC-72, Experimental Heat Transfer 11 (1998) 121.

[13] H. Sun, C.F. Ma, W. Nakayama, Local characteristics of convective heat transfer from simulated microelectronic chips to impinging submerged round water jets, Journal of Electronic Package 115 (1993) 71.

[14] Y.S. Xu, Z.Y. Guo, Heat wave phenomena in IC chips, International Journal of Heat and Mass Transfer 38 (1995) 2919–2922.

[15] F.P. Incropera, Convection heat transfer in electronic equipment cooling, ASME J. Heat Transfer 110 (1988) 1097.

[16] Y. Jaluria, Interaction of natural convection wakes arising from thermal sources on a vertical surface, ASME J. Heat Transfer 107 (1985) 883.

[17] S.B. Sathe, Y. Joshi, Natural convection arising from a heat generating substrate-mounted protrusion in a liquid-filled two-dimensional enclosure, International Journal of Heat and Mass Transfer 34 (1991) 2149–2163.

[18] K.D. Cole, Conjugate heat transfer from a small heated strip, International Journal of Heat and Mass Transfer 40 (1997) 2709–2719.

[19] R. Anderson, A. Bejan, Natural convection on both sides of a vertical wall separating fluids at different temperatures, ASME J. Heat Transfer 102 (1980) 630–635.

[20] W.M. Kays, B. Crawford, Convective Heat and Mass Transfer, McGraw-Hill, New York, 1980.

[21] F.P. Incropera, D.P. DeWitt, Fundamentals of Heat and Mass Transfer, Wiley, New York, 1996.